Highly Uniform Vertical-Cavity Surface-Emitting Lasers Integrated with Microlens Arrays

S. Eitel, S. J. Fancey, H.-P. Gauggel, K.-H. Gulden, W. Bächtold, *Senior Member, IEEE*, and M. R. Taghizadeh

***Abstract*—In this paper, work is described on the fabrication of highly uniform 8 × 8 arrays of GaAs–AlGaAs vertical-cavity surface-emitting lasers (VCSEL's). Oxide-confined VCSEL arrays show an average threshold current of 0.74±0.02 mA, an average output power of 2.05±0.03 mW at 8 mA and an average power conversion efficiency of 14.3%. Their wavelength is measured to be 967±0.35 nm over the array. In addition, we describe the alignment and integration of these device arrays with arrays of refractive microlenses to allow beam shaping typically required in system applications.**

***Index Terms*—Microlens arrays, optical interconnections, vertical-cavity surface-emitting lasers.**

I. Introduction

THERE IS increasing interest in the use of optical techniques for the transfer of digital data within electronic systems. A key component of future optoelectronic interconnects will be surface-normal arrays of devices that will allow the exploitation of three-dimensional interconnects, taking advantage of the possibilities of high space-bandwidth connections allowed by optics [1]. Vertical-cavity surface-emitting lasers (VCSEL's) offer high bandwidth, high efficiency emission of optical data with good contrast, and excellent beam quality. Many workers are developing arrays of devices with powers in excess of 1 mW per device to provide the sources for future interconnect systems [2], [3].

In this letter, we describe 8 × 8 arrays of VCSEL's designed for the types of system applications referred to above, stressing in particular the uniformity of the electrical and optical parameters of these arrays. We further describe a simple and effective technique for the integration of these VCSEL arrays with arrays of refractive microlenses using a combination of optical and mechanical methods.

II. Array Fabrication and Characteristics

The VCSEL's described here were designed for top emission at 960-nm wavelength. They were grown by metal–organic vapor phase epitaxy (MOVPE) on an n-type GaAs substrate. The structure consists of a one-wavelength AlGaAs cavity with three central $In_{0.13}Ga_{0.87}As$ quantum wells, sandwiched between two distributed Bragg reflectors (DBR's) of alternating GaAs and $Al_{0.9}Ga_{0.1}As$ layers with linear heterointerface grading. Twenty-one and 30.5 mirror pairs form the top (p-doped) and bottom (n-doped) DBR's, respectively. The VCSEL's were processed both as air–post and as oxide-confined devices in an 8 × 8 array configuration [see Fig. 1]. The main processing steps include the formation of a common n-contact (AuGeNi), individual p-contact rings (PtTiPtAu), and dry etching (ECR) of circular mesas. For the electrical isolation, a 1.2-μm-thick Si_3N_4 layer is deposited and subsequently reopened on top of the mesas. Finally, the electrical wiring of

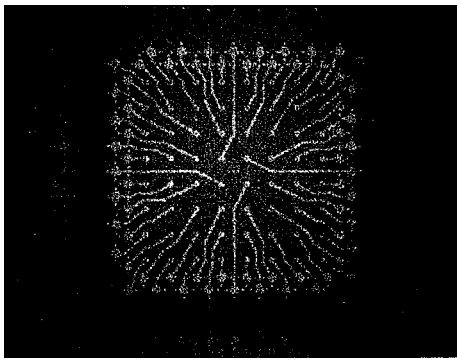

(a)

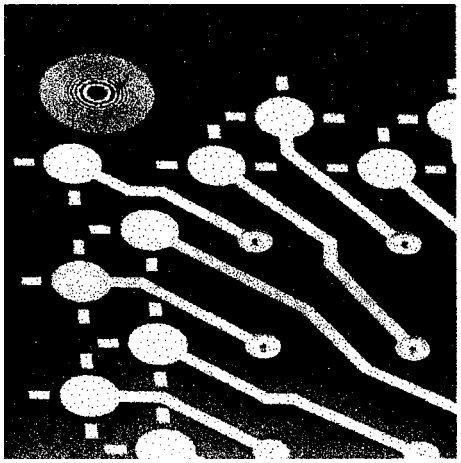

(b)

Fig. 1. (a) High-resolution image of VCSEL array. The individual devices may be seen, as may the reflective Fresnel zone plates for alignment of the microlens array in three of the array corners. (b) Further magnified image showing one of the three Fresnel zone plates deposited with the top-layer metal on the VCSEL array.

Manuscript received September 16, 1999; revised January 24, 2000. This work was supported by the European Union under the ESPRIT Proactive Scheme Microelectronics Advanced Research Initiative Opto-Cluster Project SPOEC. This work was supported in part by the BBW, Bern, under Contract 96.0108.

S. Eitel, H.-P. Gauggel, and K.-H. Gulden are with the Centre Suisse d'Electronique et de Microtechnique, CH-8048 Zürich, Switzerland.

W. Bächtold is with the Electrical Engineering Department, Swiss Federal Institute of Technology (ETHZ), CH-8092 Zürich, Switzerland.

S. J. Fancey and M. R. Taghizadeh are with the Department of Physics, Heriot-Watt University, Edinburgh EH14 4AS, Scotland, U.K.

Publisher Item Identifier S 1041-1135(00)03610-7.

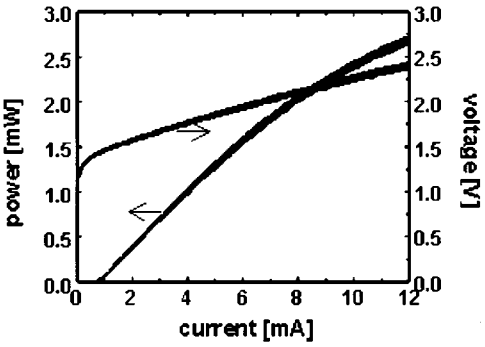

Fig. 2. DC characteristics of the 64 individual devices of an oxide confined 8×8 VCSEL array.

the p-contact rings to the corresponding bond pads is deposited. For the oxide-confined arrays, an additional 25-nm $Al_{0.98}Ga_{0.02}As$ oxidation layer embedded in the second $Al_{0.9}Ga_{0.1}As$ layer above the cavity was oxidized in a wet-oxidation furnace at 425 °C to form the buried current aperture. The pitch between the individual devices is 250 μm and the whole VCSEL array occupies an area of 2.8×2.8 mm^2.

The main dc characteristics of the VCSEL arrays were measured on wafer level. For a nonoxidized array with devices with 10-μm diameter of the p-contact opening and 14-μm mesa diameter, the values are as follows: mean threshold current: 2.65±0.05 mA (±2%); mean threshold voltage: 1.88±0.01 V (±0.5%); output power: 1.25±0.02 mW (±1.5%) at 8 mA. The average peak power conversion efficiency is 6.3%. The VCSEL's emit at 956 nm with a maximum variation of 0.7 nm. For an oxidized VCSEL array, Fig. 2 shows the output power and voltage versus current characteristics of all 64 individual devices (8-μm oxide aperture diameter) and illustrates the performance progress compared to the nonoxidized VCSEL array. The average threshold current of 0.74±0.02 mA (±3%) is reduced by more than a factor three and the average output power of 2.05±0.03 mW (±1.5%) at 8 mA is almost doubled. Since the resistances are similar (80 Ω for the oxidized, 79 Ω for nonoxidized VCSEL's at 8 mA), the reduced mean threshold current implies a reduced mean threshold voltage of 1.44±0.01 V (±0.7%), which is only 140 mV above the photon potential. The average power conversion efficiency (not shown) peaks around 4 mA with a value of 14.3%. The mean emission wavelength for the oxidized array is 967 nm for individual operation at 1 mA with a difference between the maximum and minimum value of only 0.7 nm (±0.07%).

The performance progress for oxidized devices is generally attributed to the efficient carrier injection into the active region and the low-loss index guiding due to the oxide aperture. Both the oxidized and nonoxidized VCSEL array show a remarkable uniformity of electrical and optical parameters, which can be attributed to small thickness variations of the MOVPE grown epitaxial layer structure, uniform wafer processing, and small variations in the oxide aperture diameter across the array area.

III. Integration of VCSEL's with a Microlens Array

The integration of VCSEL's with microlenses allows us to alter the divergence of the emitted beams to match system requirements and, furthermore, has the considerable benefit of providing a measure of physical protection for the emitter array in the system environment.

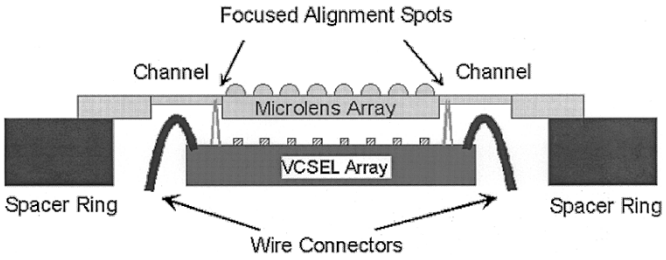

Fig. 3. Integration scheme showing the supporting ring, the channels cut in the microlens array substrate to protect bond wires, and the Fresnel lenses for lateral alignment.

An 8×8 array of refractive microlenses has been fabricated in fused silica using thermal reflow of photoresist followed by mask erosion [4]. The lenses are on a 250-μm pitch, to match the VCSEL array described above. They have a sag of 7.9 and a diameter of 160 μm resulting in a focal length of 909 μm in air. Following fabrication, both surfaces have been antireflection coated.

The patented scheme [5] developed for the integration of the two components is illustrated in Fig. 3. The vertical spacing of the microlens array from the VCSEL chip emitters is achieved by placing a precisely machined ring around the chip itself. To produce an $f/6.69$ beam using the microlenses described above, we would require a standoff from the VCSEL surface of 145 μm, for a microlens substrate thickness of 505 μm. The plastic supporting ring may be positioned approximately and glued into position.

The critical lateral alignment of the microlens array is achieved using reflective Fresnel zone plates deposited as part of the top-level metallization mask of the VCSEL fabrication [6]. These zone plates are positioned in the corners of the VCSEL array, as shown in Fig. 1(b). The focal length of the diffractive lenses is chosen to produce a focus near the top surface of the microlens array, in which corresponding alignment marks are positioned. Upon illumination at a wavelength of 633 nm, for which the reflective alignment lenses were designed, it is straightforward to bring the alignment spots and markers into coincidence, as shown in Fig. 3. By using three Fresnel lenses, we can control rotational as well as translational alignment. The estimated lateral alignment precision of this technique is $\sim$2 μm. The microlens array is attached to the supporting ring using UV-curing optical adhesive, cured only following final adjustment. We have found that it is possible to subsequently remove the microlens array without damage to the VCSEL chip.

To protect the bond wires on the VCSEL assembly, we cut 100–200-μm-deep channels in the substrate side of the microlens array using a dicing saw. The 510-μm-thick substrate has shown no evidence of stress or fracture in normal handling following the cutting of these grooves. Note that since vertical positioning is produced independently (by the supporting ring), the focal plane of the reflective beam is not critical. Fig. 4 shows a section of the integrated VCSEL/microlens array, viewed through the microlenses.

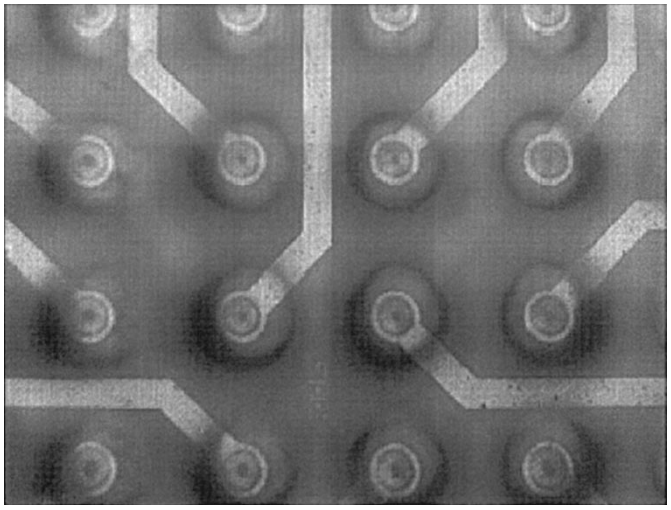

Fig. 4. Part of the VCSEL array viewed through the microlens array after attachment.

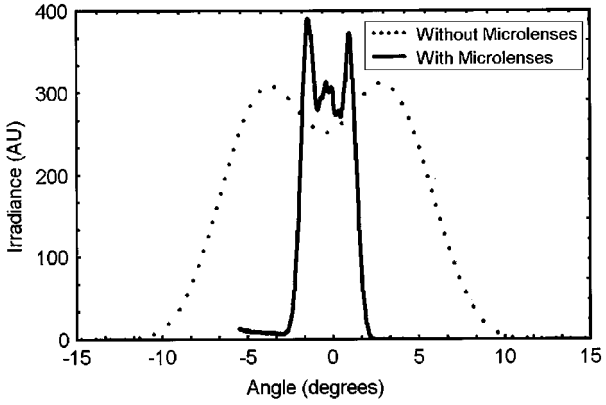

Fig. 5. The far-field beam profile of a nonoxidized VCSEL operating at 8-mA current shown before and after the integration of the VCSEL array with microlenses. The resulting reduction in the divergence may be clearly seen.

A typical beam from our system experiments [7] is shown in the far-field irradiance profile of Fig. 5, before and after shaping by the integration of microlenses. The decrease in the divergence of the VCSEL emission from 12.6° full-width at half-maximum (FWHM) to 5.1° FWHM, corresponding to $f/6.6$ ($1/e^2$ points) may be clearly seen. The distribution of the divergence across the whole array is 13.0±0.7° without attached microlenses and 4.9±0.7° after integration with the microlens array. Both of these FWHM uniformity measurements were made at a VCSEL current of 8 mA.

IV. Conclusion

In this letter, we have described both significant progress in the manufacture of uniform high-power 8×8 VCSEL arrays and a practical technique for integration of the VCSEL's with microlens arrays to adapt the divergent sources for system applications. The packaged combination is of interest as a source in digital optoelectronic interconnects and other areas.

Acknowledgment

The authors would like to thank A. C. Walker, N. Ross, O. Glatigny, and other colleagues in the SPOEC partner institutions for their contribution to the work reported here.

References

[1] D. A. B. Miller, "Physical reasons for optical interconnection," *Int. J. Optoelectron.*, vol. 11, no. 3, pp. 155–168, 1997.

[2] R. King, R. Michalzik, C. Jung, M. Grabherr, F. Eberhard, R. Jäger, P. Schnitzer, and K. J. Ebeling, "Oxide confined 2D VCSEL arrays for high-density inter/intra-chip interconnects," *Proc. SPIE—Int. Soc. Opt. Eng.*, vol. 3286, pp. 64–71, 1998.

[3] K. M. Geib, K. D. Choquette, H. Q. Hou, and B. E. Hammons, "Uniformity and performance of selectively oxidized VCSEL arrays," *Proc. SPIE—Int. Soc. Opt. Eng.*, vol. 3286, pp. 72–75, 1998.

[4] M. C. Hutley, "Refractive lenslet arrays," in *Micro-Optics: Elements, Systems and Applications*, H. P. Herzig, Ed. London, U.K.: Taylor and Francis, 1997, pp. 127–152.

[5] "Method for the alignment of lens arrays," U.K. Patent 9 812 972.9, 1998.

[6] G. C. Boisset, B. Robertson, W. S. Hsiao, M. R. Taghizadeh, J. Simmons, K. Song, M. Matin, D. A. Thompson, and D. V. Plant, "On-die diffractive alignment structures for packaging of microlens arrays with 2-D optoelectronic device arrays," *IEEE Photon. Technol. Lett.*, vol. 8, pp. 918–920, July 1996.

[7] A. C. Walker, M. P. Y. Desmulliez, M. G. Forbes, S. J. Fancey, G. S. Buller, M. R. Taghizadeh, J. A. B. Dines, C. R. Stanley, G. Pennelli, A. R. Boyd, P. Horan, D. Byrne, J. Hegarty, S. Eitel, H.-P. Gauggel, K.-H. Gulden, A. Gauthier, P. Benabes, J. L. Gutzwiller, and M. Goetz, "Design and construction of an optoelectronic crossbar switch containing a terabit/s free-space optical interconnect," *IEEE J. Select. Topics Quantum Electron.*, vol. 5, pp. 236–249, Feb. 1999.